except in cases of severe supply ischemia (2,3). Although this duration is valuable for stress echocardiography, it seems to be short to use for ischemic memory imaging. However, a latent decrease in myocardial contractility due to ischemia may continue for a while even after normalization of the strain profile.

In the present results, brief afterload augmentation allowed reappearance of PSS that had disappeared after transient ischemia. We believe that the relative decrease in ε_{ES} is a main mechanism of the reappearance of PSS during afterload augmentation. The present study suggests that this technique can reveal concealed myocardial dysfunction and may be useful for ischemic memory imaging via speckle-tracking echocardiography.

Kasumi Masuda, PhD
Toshihiko Asanuma, MD, PhD*
Daisuke Sakurai, MSc
Satoshi Nakatani, MD, PhD
*Division of Functional Diagnostics
Department of Health Sciences
Osaka University Graduate School of Medicine
1-7 Yamadaoka, Suita
Osaka 565-0871
Japan
E-mail: toshi@sahs.med.osaka-u.ac.jp
Twitter: #JACCIMG, #cvimaging, #cvEcho

https://doi.org/10.1016/j.jcmg.2018.03.022

Please note: This research was supported by Japan Society for the Promotion of Science Grant-in-Aid for Scientific Research (JSPS KAKENHI grant number JP09J03474). The authors have reported that they have no relationships relevant to the contents of this paper to disclose.

REFERENCES

1. Masuda K, Asanuma T, Taniguchi A, et al. Assessment of dyssynchronous wall motion during acute myocardial ischemia using velocity vector imaging. J Am Coll Cardiol Img 2008;1:210–20.

2. Asanuma T, Uranishi A, Masuda K, et al. Assessment of myocardial ischemic memory using persistence of post-systolic thickening after recovery from ischemia. J Am Coll Cardiol Img 2009;2:1253–61.

3. Asanuma T, Fukuta Y, Masuda K, et al. Assessment of myocardial ischemic memory using speckle tracking echocardiography. J Am Coll Cardiol Img 2012;5:1–11.

4. Leone BJ, Norris RM, Safwat A, et al. Effects of progressive myocardial ischaemia on systolic function, diastolic dysfunction, and load dependent relaxation. Cardiovasc Res 1992;26:422–9.

Early Changes in Myocardial Mechanics Detected by 3-Dimensional Speckle Tracking Echocardiography in Patients Treated With Low Doses of Anthracyclines

Cancer therapy-related cardiac dysfunction (CTRCD) represents an important cause of morbidity and mortality; early detection along with cardioprotection are fundamental to improve prognosis (1). However, usual diagnostic parameters have low sensitivity, increasing interest for early markers of CTRCD (1). A 3-dimensional speckle tracking echocardiography (3D-STE) has revealed more consistent data than a 2-dimensional (2D) technique and may prove to be more accurate in patients undergoing chemotherapy (2). This prospective study investigated myocardial deformation using 3D-STE in patients with breast cancer treated with low doses of anthracyclines to identify early markers of cardiotoxicity.

Patients >18 years of age, newly diagnosed with breast cancer, and scheduled for chemotherapy with anthracyclines were eligible. Exclusion criteria included previous chemotherapy or radiotherapy, inadequate echocardiographic imaging (>2 non-visualized segments) and a left ventricular ejection fraction (LVEF) <55% before chemotherapy. Patients underwent a comprehensive echocardiogram and collection of ultrasensitive troponin I (US-TnI) during the following 3 stages: at baseline and after non-liposomal doxorubicin cumulative dosages of 120 and 240 mg/m^2. We analyzed the LVEF (Simpson's method), 2D global longitudinal strain (GLS), and 2D midpapillary radial strain (RS); for 3D-STE, we measured 3D-GLS, 3D-global RS, global circumferential strain (3D-GCS), and global area strain (3D-GAS) along with rotation, twist, and torsion. Variables were compared among evaluation stages using generalized estimating equations with normal distribution and identity link function followed by multiple Bonferroni comparisons. Due to the asymmetric distribution, for US-TnI, the logarithmic function was used.

A total of 47 patients were eligible for the study, with 3 exclusions (2 due to inadequate echocardiographic images and 1 noncardiac-related death). Forty-four female patients 48.7 ± 10.8 years of age were evaluated, with results summarized in **Table 1**. The mean LVEF was unchanged during treatment; however, the 2D-GLS decreased only after the 240 mg/m^2 dose ($p = 0.001$), with no changes after a lower dosage of doxorubicin (120 mg/m^2). The 2D-RS was similar during both stages. After a dose of 240 mg/m^2 of doxorubicin, 3D-STE detected changes in most myocardial deformation parameters: 3D-GLS, 3D-global RS, 3D-GCS, and 3D-GAS; no changes were observed for rotation, torsion, or twist. After a lower dose of doxorubicin, the only parameters that changed were 3D-GCS ($p = 0.021$) and 3D-GAS ($p < 0.001$). Twenty patients (45%) presented with a US-TnI of >34 pg/ml after a doxorubicin dose of 240 mg/mg^2 ($p = 0.001$); however, a lower doxorubicin dose produced no change in US-TnI.

TABLE 1 Results for the 3 Evaluation Stages

	Baseline	120 mg/m²	p Value*	240 mg/m²	p Value†
LVEF	0.64 ± 0.02	0.63 ± 0.03	–	0.63 ± 0.03	0.218
2D speckle tracking, %					
2D-GLS	−18.2 ± 1.3	−17.9 ± 1.2	0.103	−17.4 ± 1.3	0.001
2D-RS	38.4 ± 9.1	38.4 ± 8.7	–	36.1 ± 12.8	0.47
3D speckle tracking, %					
3D-GLS	−16.4 ± 1.9	−15.9 ± 1.9	0.333	−14.8 ± 1.8	<0.001
3D-GRS	31.4 ± 12.6	26.9 ± 11.5	0.156	25.2 ± 11.6	0.03
3D-GCS	−34.3 ± 4.8	−32.2 ± 4.5	0.021	−30.8 ± 4.4	<0.001
Twist, °	5.7 ± 2.5	5.3 ± 3.1	–	4.7 ± 2.4	0.175
Torsion, °/cm	2.6 ± 1.4	2.5 ± 1.6	–	2.2 ± 1.3	0.43
Rotation, °	5.5 ± 2.8	4.8 ± 2.1	–	4.5 ± 2.2	0.097
3D-GAS, %	−45.9 ± 3.8	−43.4 ± 4.2	<0.001	−39.9 ± 3.3	<0.001
US-TnI, pg/ml	12.0 ± 0.6	16.6 ± 8.2	0.509	40.7 ± 27.6	<0.001
US-TnI >34 pg/ml	0 (0)	1 (2)	0.96	20 (45)	0.001

Values are mean ± SD or n (%). *Changes after doxorubicin 120 mg/m² compared with baseline (multiple Bonferroni comparisons applied if statistical significance after 240 mg/m²). †Changes after doxorubicin 240 mg/m² compared with baseline.

2D = 2-dimensional; 3D = 3-dimensional; GAS = global area strain; GCS = global circumferential strain; GLS = global longitudinal strain; GRS = global radial strain; LVEF = left ventricular ejection fraction; US-TnI = ultrasensitive troponin I.

Myocardial deformation analysis using 3D-STE has been shown to be reliable and reproducible to assess LV mechanics in various clinical conditions (2). However, this technique has been poorly explored in the scenario of CTRCD. In the present study, after a cumulative dosage of 240 mg/m² of doxorubicin, changes in almost all 3D-STE indexes were observed, implying that abnormalities are present in all directions of myocardial contraction. Interestingly, 3D-GCS and -GAS were the only parameters that changed at an earlier stage, suggesting improved sensitivity for early detection of chemotherapy-related changes. Recent research has evaluated patients under treatment with anthracyclines, demonstrating the potential superiority of 3D-GCS and -GAS compared with other echocardiographic parameters for the subclinical diagnosis of cardiotoxicity (3); however, these patients were evaluated after a greater cumulative anthracyclic dosage, with the association of traztuzumab or radiotherapy. Changes in torsion and twist rate were observed with the 2D technique after anthracyclic treatment (4); however, 3D-STE analysis did not confirm these findings. Finally, despite its confirmed value after a high dosage of anthracyclines, US-TnI was not useful to detect early changes in patients with breast cancer.

Some limitations must be pointed out, namely, the small sample size, research performed in a single center, and the low 3D-STE volume rate (20 to 30 volumes/s). Moreover, long-term follow-up is necessary to determine whether 3D-STE changes might correlate with clinical outcomes or subsequent LVEF reduction.

In conclusion, this analysis of myocardial mechanics using 3D-STE in patients with breast cancer treated with anthracyclines detected early changes in 3D-GCS and -GAS after very low doses of doxorubicin, representing a promising technique for CTRCD.

Rafael B. Piveta, MD*
Ana Clara T. Rodrigues, MD, PhD
Marcelo L.C. Vieira, MD, PhD
Cláudio H. Fischer, MD, PhD
Tania R. Afonso, RN
Edgar Daminello, MD, PhD
Felipe M. Cruz, MD, PhD
Tatiana F.G. Galvão, MD, PhD
Marcelo Katz, MD, PhD, MHS
Samira S. Morhy, MD, PhD

*Hospital Israelita Albert Einstein
Av. Albert Einstein 627/701
Morumbi
São Paulo
SP 05652-900
Brazil
E-mail: rafael.piveta@einstein.br
Twitter: @rbpiveta

https://doi.org/10.1016/j.jcmg.2018.04.014

Please note: The authors have reported that they have no relationships relevant to the contents of this paper to disclose.

REFERENCES

1. Plana JC, Galderisi M, Barac A, et al. Expert consensus for multimodality imaging evaluation of adult patients during and after cancer therapy: a report from the American Society of Echocardiography and the European Association of Cardiovascular Imaging. J Am Soc Echocardiogr 2014;27:911–39.

2. Saito K, Okura H, Watanabe N, et al. Comprehensive evaluation of left ventricular strain using speckle tracking echocardiography in normal adults: comparison of three-dimensional and two-dimensional approaches. J Am Soc Echocardiogr 2009;22:1025–30.

3. Santoro C, Arpino G, Esposito R, et al. 2D and 3D strain for detection of subclinical anthracycline cardiotoxicity in breast cancer patients: a balance with feasibility. Eur Hear J Cardiovasc Imaging 2017;18:930–6.

4. Motoki H, Koyama J, Nakazawa H, et al. Torsion analysis in the early detection of anthracycline-mediated cardiomyopathy. Eur Heart J Cardiovasc Imaging 2012;13:95–103.

Focus on the Perimeter and Skip the Balloon

Can Atrial Septal Defect Be Percutaneously Closed Without Balloon Sizing in the Era of 3-Dimensional Echocardiography?

When technically feasible, device closure is the treatment of choice for ostium secundum atrial septal defect (ASD) (1). Three-dimensional (3D) transesophageal echocardiography (TEE) has recently emerged as a powerful tool that can accurately guide device selection in ASD closure (2,3). We aimed to investigate the utility of direct 3D TEE device sizing on the basis of the ASD perimeter.

As part of a single-center prospective observational study, 49 consecutive adults (73% women; mean age 50 ± 16 years) after successful transcatheter closure of a single ASD were enrolled between 2014 and 2016. Interventions were performed while patients were under general anesthesia, through a femoral venous access, using an Amplatzer Septal Occluder (St. Jude Medical, Inc., Little Canada, Minnesota). The actual size of the occluder implanted was chosen on the basis of the conventional strategy (i.e., 2-dimensional TEE with complementary balloon sizing). Blinded 3D TEE images were acquired before each procedure (Vivid 9 ultrasound machine, 6VT-D transducer, 3 to 8 MHz, GE Healthcare, Milwaukee, Wisconsin) for post-procedural processing. In particular, ASD perimeter was manually traced in a multiplanar en face view reconstructions in the end-systolic frame when it appeared largest. Maximum diameter (d_{max}), minimum diameter (d_{min}), and perimeter (P) were measured by 2 independent observers (**Figure 1A**). Defect shape was categorized as round or oval on the basis of the circular index (d_{max}/d_{min}), while considering defects with the ratio <1.5 as round.

Mean d_{max} was 15.7 ± 5 mm, mean d_{min} was 11.7 ± 3.9 mm, and mean P was 45.8 ± 14.2 mm. A total of 34 defects (69%) were classified as round. Mean balloon-stretched diameter and mean occluder size did not differ significantly (18.9 ± 4.9 mm and 18.9 ± 5.4 mm,

FIGURE 1 Occluder Size Estimation on the Basis of ASD Perimeter

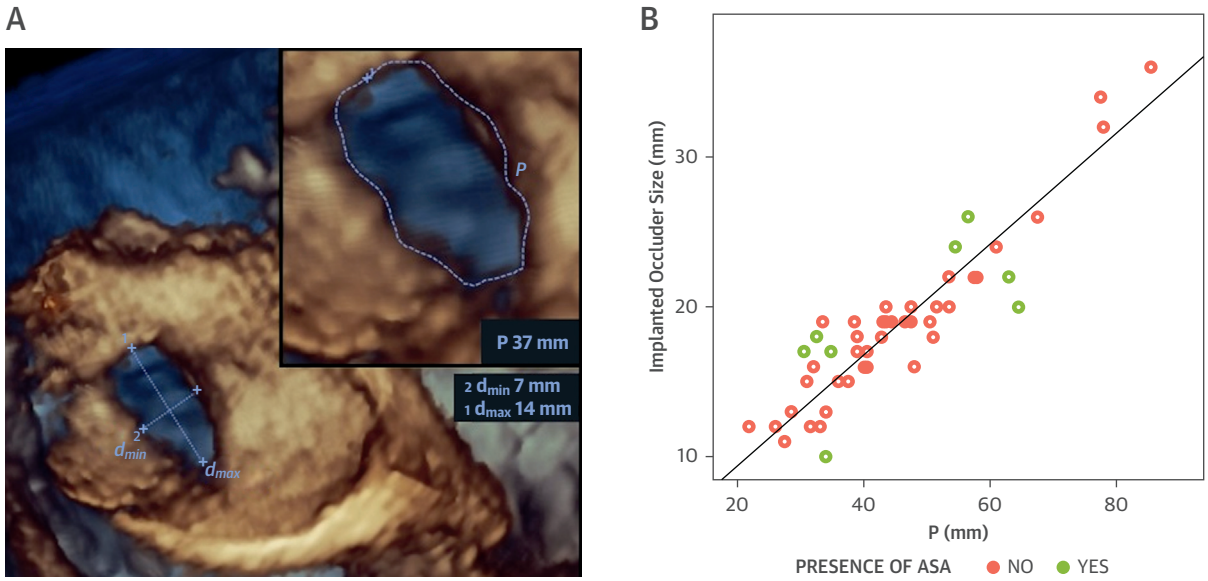

(A) A 3-dimensional (3D) transesophageal echocardiography (TEE), full volume en face view reconstruction. Atrial septal defect (ASD) measurement: maximal diameter (d_{max}), minimal diameter (d_{min}), and perimeter (P). **(B)** Linear correlation between the implanted occluder size and atrial septal defect perimeter (P) measured by 3-dimensional transesophageal echocardiography; **pink dots** represent subjects without atrial septal aneurysm (ASA) (n = 41), and **green dots** represent subjects with atrial septal aneurysm (n = 8).